Scanning Tunneling Microscopic Studies of Epitaxial Films of Polyurethane, Polyester, and Polysiloxane Formed during Step Polymerization

Masahito Sano,* Mats O. Sandberg, Nobusuke Yamada, and Susumu Yoshimura

π-Electron Materials Project—JRDC, 43 Miyukigaoka, Tsukuba, Ibaraki 305, Japan

Received October 4, 1994; Revised Manuscript Received December 28, 1994[⊗]

ABSTRACT: Crystalline films of poly(hexamethylene–hexamethylenediurethane) were found to grow on the basal plane of graphite during polyaddition of diol and diisocyanate in a homogeneous solution containing a graphite substrate. Direct observations by scanning tunneling microscopy indicate that the film has been grown epitaxially. Also, an epitaxial film of poly(hexamethylene sebacate), an aliphatic polyester having the same number of bonds per monomeric unit as the polyurethane, was grown on the graphite surface during polycondensation of diol and dichloride. These results demonstrate that step polymerization induces epitaxy of polymers during polymerization. Then, the same polycondensation procedures were applied to study the films of an aromatic polyester, poly(hexamethylene terephthalate), and a polyester containing a triple bond, poly(butynyl sebacate) on graphite. The aromatic ring and the triple bond can be considered as the structural "kinks" on the aliphatic backbones that cause a misfit with a polyethylene-like repeat of the graphite hexagonal lattice. Formation of epitaxial films of these polyesters indicates the importance of having molecular structures capable of forming a close packed state in two dimensions for this epitaxial growth. Lastly, ring-opening polymerizations of cyclic dimethylsiloxanes were performed with the presence of a graphite substrate either in a good solvent at room temperature or in melt at 160 °C. Formation of crystalline films even at the temperatures much higher than the melting point of bulk polymer (−42 °C) and entropically driven polymerization of siloxanes suggest the two-dimensional nature of the crystallization process. On the basis of the present results and the previous studies, a mechanism of the late stage of epitaxial growth induced by polymerization is proposed.

Introduction

Recently, crystalline films of polymers were found to grow epitaxially on a solid surface during chain polymerization in solution.[1] It has been shown that the *in situ* polymerization process is absolutely necessary for this crystalline growth. Simply placing a solid substrate in a monomer or a polymer solution under the same conditions has not given any crystalline films. Thus, this phenomenon differs from an ordinary absorption or crystallization process and epitaxy of polymers during solution polymerization is termed *polymerization-induced epitaxy* (PIE).

Performing anionic or cationic ring-opening polymerization of cyclic ethers in the vicinity of the basal plane of graphite resulted in a polymorphic growth of polyethers on the graphite surface.[2] Ring-opening polymerization of cyclic lactones produced the crystalline films of polylactones[3] and that of cyclic lactam resulted in a nylon film on the graphite.[4] The same process was also successful in growing an epitaxial film of poly(vinylidene chloride) on graphite by radical polymerization of vinylidine chloride.[5] Crystalline films of stereoregular poly(amino acids) were obtained through ring-opening polymerization of *N*-carboxy-α-amino acid anhydrides.[6]

These studies indicate that PIE is not in accord with the known results of adsorption or crystallization of polymers in solution or melt.[7–9] As stated above, if a substrate surface was only immersed in a preformed polymer solution (without polymerization) under the same physical conditions as PIE, no film growth was observed. In some cases, the solvent itself was a monomer and no epitaxial film resulted, even in melt. Thus, even though adsorption may have an effect at the beginning, it is not the only process responsible for PIE. At an early stage of polymerization, all reactants and products of reactions are completely dissolved in the solvents. Subsequent epitaxial growth takes place regardless of whether growing polymers stay dissolved in the mixtures or precipitate in the middle of reactions. Also, we can vary the concentration and temperature of polymerization over a wide range without having difficulty in forming the crystalline film (the film size and the coverage may vary). These observations suggest that PIE is not a late crystallization process of solution-grown compounds.

We also found no particular relationship between PIE and the details of chain polymerization. A film formation is independent of the type of initiator used and of the propagation mechanisms of chain polymerization.[10] No experimental data suggesting a direct contribution of the graphite substrate to the chemical reactions are observed. A wide variety of working reactions also indicates that PIE is not a kind of surface-catalyzed reaction or topochemical reaction of aggregated monomers. This view is further supported by the present study involving step polymerization.

The previous studies have revealed a variety of molecular structures that can be grown by PIE on the graphite surface. These include all *trans*, planar zigzag conformations as well as a glide conformation containing both *trans* and *gauche* moieties. More complex structures, such as hydrogen-bonded networks of nylon-6 and poly(glycine) resembling a β-sheet, are also observed. The basal plane of graphite consists of hexagonally packed carbon atoms with two principal crystallographic directions $\langle 10\bar{1}0 \rangle$ and $\langle 2\bar{1}\bar{1}0 \rangle$. A unit repeat in the

[⊗] Abstract published in *Advance ACS Abstracts,* February 15, 1995.

0024-9297/95/2228-1925$09.00/0

direction of $\langle 2\bar{1}\bar{1}0\rangle$ is very close to the advancing distance of the polyethylene-like backbone along its fiber axis. Although the neutral, flat surface of graphite having a polyethylene-like array may be a major reason for the rich variety of epitaxial structures, it is also true that the PIE process is not selective on a detail of molecular structures.

These epitaxial growths of polymers were confirmed and analyzed by direct observations of molecular films using scanning tunneling microscopy (STM).[11] This was also one of the primary reasons for the use of graphite as a substrate. After the PIE process, the graphite surface is typically covered by adsorbed amorphous layers of the solution-grown polymers as well as crystalline layers. If solvent is available for solution-grown polymers, the surface can be washed thoroughly to remove either type of polymer. It turns out, however, that the first few crystalline layers on the surface cannot be washed away under the conditions that bulk polymers are normally dissolved, probably due to a difficulty in solvating a highly crystalline film attached to a solid surface. Having a thickness of 1 nm or less and close packing of molecules in a crystalline form, there is no problem in reproducibly imaging the polymer molecules in near-atomic resolution by STM.

The present study is undertaken to investigate the feasibility of step polymerization for PIE and to gain insight into the PIE mechanism. Step polymerization is attractive for a vast number of commercially available monomers. A wide selection of monomers also implies that the unit cell size can be controlled by a suitable choice of spacer elements while the same functional unit is kept in a film structure. This is particularly helpful for an interpretation of STM images of complex polymers. Also, a stepwise growth of chains by addition of a reacting segment having an arbitrary number of monomeric units in step polymerization should tell us more about the crystallization process than a monomer-wise addition in chain polymerization.

We first describe a detailed study of aliphatic polyurethane film made by polyaddition of diol and diisocyanate. Hydrogen bonding and lattice matching guide us to identify the chain conformation, the chain packing, and most importantly, the orientation of polymer lattice relative to the substrate lattice in an atomic scale. Then, an aliphatic polyester film grown by polycondensation is discussed. We have chosen the monomers so that the resulting polyester has approximately the same monomer length as the polyurethane to aid in STM image analyses. A difficulty in STM analysis of polymers containing spatially nonsymmetric functional units like an ester group was expected from the previous study of polylactones.[3]

Having shown that step polymerization works for PIE by the aliphatic polymers, we proceed to study polyesters containing an aromatic ring or a triple bond in its chain backbone. These functional groups in the polymers represent a kind of structural "kink" in the polyethylene-like backbones and do not "fit" well on the graphite hexagonal lattice which has a polyethylene-like repeat. These films not only indicate a possibility of functionalization of epitaxial films but suggest a condition on the molecular structures that can be grown epitaxially by PIE as well.

Lastly, we present a result of the polysiloxane study, where the PIE process has been performed at temperatures as high as 200 °C above the melting point of bulk polymer. On the other hand, this polymerization reaction is known to be entropically driven with no change in enthalpy.[10] This competition of entropy between crystallization and polymerization supports a tentative model of film growth by PIE proposed at the end of the section.

Experimental Sections

General Procedure for PIE and Washing. Conventional polymerization reactions[10] are employed but are limited to solution polymerization to avoid the complication of having two surfaces in the case of interfacial polymerization. A freshly cleaved highly oriented pyrolytic graphite (HOPG) is immersed in a mixture containing monomers and other reagents necessary for polymerization at a desired temperature. Although the reaction is started in a conventional way, we have found that it is not important whether the graphite substrate is added before or after initiation as long as it is present at an early stage of reaction. After a desired reaction time, the graphite is taken out of the mixture. Then, the graphite surface is washed by good solvents of polymers as well as other common solvents for all possible products, heating to high temperatures if necessary. Typically, we use several kinds of solvents, refreshing each solvent a few times a day over a period of weeks. Because HOPG allows very little adsorption by most organic compounds, the HOPG surface is free of polymers after this washing if the polymer is only adsorbed and is not epitaxially grown.

Solution Polymerization. Poly(oxyhexamethyleneoxycarbonyliminohexamethyleneiminocarbonyl) ((6,6)urethane) was synthesized by adding 6.3 mmol of 1,6-hexanediol to a mixture containing an equimolar amount of 1,6-diisocyanohexane with a catalytic amount of dibutyltin dilaurate and a freshly cleaved HOPG in dimethyl sulfoxide over a few minutes at 60 °C. The polymer started to precipitate as the reaction proceeded. After 1 h, ethanol was added to the mixture and HOPG was taken out of the mixture. Hot *m*-cresol was mainly used to repeatedly wash HOPG. Other washing solvents included water, ethanol, chloroform, tetrahydrofuran, and hexane.

The polyesters were synthesized by the Schotten-Baumann reaction in one phase using pyridine as base. After pyridine was added to a mixture containing 2 mmol each of monomers and HOPG at −15 °C, the mixture was heated to 60 °C for 3 h before HOPG was taken out. Dry tetrahydrofuran was used as solvent for the synthesis of poly(oxysebacoyloxyhexamethylene)((6,10)ester) from 1,6-hexanediol and sebacoyl chloride. The polyether remained soluble over the entire process. 1,6-Hexanediol and terephthaloyl chloride were used to obtain poly(oxyterephthaloyloxyhexamethylene) ((6,T)ester). A 1:2.7 mixture of tetrahydrofuran:chloroform was used for the synthesis of poly(oxy(2-butynyl)oxysebacoyl) ((butyne,10)-ester) from 2-butyne-1,4-diol and sebacoyl chloride. Mostly chloroform and tetrahydrofuran were used to wash HOPG, together with water, ethanol, acetone, and hexane.

Poly(dimethylsiloxane) (PDMS) was prepared by two different synthetic methods with the graphite substrate in the reaction mixture. Anionic polymerization of hexamethylcyclotrisiloxane (D3) was initiated by *n*-butyllithium in a 50% toluene solution at room temperature and was terminated with trimethylchlorosilane.[12] Also, neat octamethylcyclotetrasiloxane (D4) was polymerized with a trace amount of wet potassium hydroxide at 160 °C.[13] While both reactions yielded nominally identical PDMS, they differed considerably in the reaction mechanism involving macrocyclization as well as the composition of the end groups. After the reaction, the film-covered graphite was washed repeatedly with toluene, *n*-hexane, tetrahydrofuran, chloroform, ethanol, and water.

STM Imaging. The STM was operated in air at ambient condition with Pt/Ir tip. The current was typically set at 100−300 pA. A stable imaging was possible with a bias voltage of approximately 0.4−1 V in either polarity. No reproducible dependence of image feature on the bias was observed. Our homemade STM operating in the constant distance mode produces about ten images every second.[2] We have performed pixel averaging of a few seconds duration of image frames (the

image appears still without significant drift) and filtering of very high frequency noise (equivalent of white sparkles on a video) as the only image processing. Molecular images different from the bare graphite image were observed in most runs at a randomly chosen area. We continued to scan different locations on the sample surface, exchanging the tip as we changed the scan location, until the frames equivalent to about 100 final images were obtained. We retained only those images that have appeared repeatedly.

Results

Surfaces Characterized by STM and the Method of Image Analysis. For all sample surfaces, there are three types of regions that can be differentiated by STM imaging. One is a bare graphite surface. The second type produces highly regular arrays of rectilinear patterns with unit cell dimensions much larger than the graphite hexagon, believed to be the molecular film. The third type gives an unstable current and transient, unrecognizable images. These regions are commonly found next to the second type areas. The same kind of unrecognizable images were also seen on the area after the molecular film had been disturbed during scanning. Also, it was often encountered on a sample that was not washed thoroughly. A further washing reduced the number of occurrences. We think that this third region corresponds to a part of the film in an amorphous state, a residual adsorbed polymer, or a tip contaminated by the polymer segment.

In the following, we shall focus on the molecular resolution images taken from the second region, since our purpose is to show that the polymer structure has some relationship with the underlying graphite lattice. The pattern exhibited by each image can be observed over distances of a few tens to several hundred nanometers typically. A larger scale morphology of the film depends on the polymerization conditions such as concentration and temperature, probably involving PIE kinetics. A further discussion of the film morphology is, however, beyond the scope of this paper.

Presently, it is very difficult to predict the molecular structure of polymers directly from the observed STM images based on the first-principles of tunneling. Both theoretical[14,15] and our previous experiments[2,3] indicate that an appearance of adsorbate on the images depends on its orientation relative to the underlying graphite atoms and may be influenced by an interference effect of quantum waves. This means that one must specify not only the structure of the polymer lattice but also its orientation relative to the graphite lattice to model the STM images. Here, we rely on a more phenomenological method and follow the same procedure as previously described.[2] Briefly, we assume that an ethylene unit contributes least to the tunneling current compared with other chemical units. Secondly, STM is known to image every other carbon atom of the graphite surface. An identical atomic species of the polymer chain should appear differently depending on the position relative to the carbon atom of graphite. We arbitrarily assign a stronger current to the polymer atom on the strongly enhanced graphite carbon than if the same polymer atom was on the less tunneling graphite carbon. We begin the analysis by constructing a model polymer lattice on the graphite lattice. Intermolecular interactions, such as hydrogen bonding, and the known bulk structures can be used as guides to model the polymer lattice. Then, the region of stronger current on this model system, in the case of polyurethane it is where a urethane unit is situated on the enhanced graphite site, is noted. Then, the periods and symmetry of the pattern created by the predicted enhanced region are measured. The same process using other polymer lattices is repeated until these measurements compare well with the actual image.

Chemical Identification of Polyurethane Film on Graphite. Fourier transform infrared spectroscopy on any of the polymer samples presented in this paper failed to show discernible peaks of the functional units due to a small quantity of polymers and a macroscopically rough graphite surface. X-ray photoelectron spectroscopy (XPS) of the graphite surface subjected to polymerization showed a peak at 401 eV, corresponding to N_{1s} of the polymer. The O_{1s} peak at ca. 530 eV increased significantly after the polymerization (air-cleaved bare graphite always contains a slight amount of oxygen), and no peak around 486 eV from tin was observed. These support a presence of only polyurethane on the graphite surface, even after rigorous washing.

Epitaxial Structures of (6,6)urethane. There are at least four different types of reproducible STM images from the same sample surface. We present here three types of images that have been analyzed so far. One of the most frequently occurring images is shown in Figure 1a. Each region of the strong current appears as an oblique bright spot in this image. These bright spots line up to form a parallel array of straight lines. A linear alignment of less bright spots runs between the lines of bright spots. The perpendicular distance between the lines of bright spots is 21−22 Å, and the space between each spots along this line is 4.9(±0.3) Å. These values are the averages measured from all images of the similar pattern taken at the different locations on the surface.

The model that is consistent with this STM image is schematically shown in Figure 1b. All *trans*, planar zigzag chains lie on $\langle 10\bar{1}0\rangle$ of graphite and the monomeric unit is modeled to be in registry with the graphite lattice. The adjacent chain is located on next to the nearest $[10\bar{1}0]$ line. The relative orientation of the chains is such that the urethane units from each chain line in the $\langle 2\bar{1}\bar{1}0\rangle$ direction. Due to the even number of ethylene units, the all *trans* conformation requires that every other urethane unit is on the strongly tunneling graphite carbon site. Thus, the predicted pattern has the bright regions line up to form the parallel straight lines 21.3 Å (=5 × 4.263 Å, where a repeating distance of graphite cells in $\langle 10\bar{1}0\rangle$ is 4.263 Å = 3 × 1.421 Å, a graphite lattice constant). The separation between each bright region along the straight line is 4.92 Å (=2 × 2.461 Å, where a repeating length in $\langle 2\bar{1}\bar{1}0\rangle$ is 2.461 Å = $\sqrt{3}$ × 1.421 Å). A bulk study indicates all trans conformaion with a fiber period of 21.9 Å, in good agreement with this model.[16] Other urethane units that are on the less tunneling graphite atoms should appear brighter than the ethylene unit, but darker than the urethane on the enhanced graphite site, and should be located between the bright spots. Thus, this model explains the characteristic features of the STM image very well.

The second image from the polyurethane shows periods similar to those above, but with a different feature, as shown in Figure 2a. Now the bright regions are streaked, giving the appearance of elongated rods. A unit repeating zone of 22 Å width contains two bands of streaked regions, one appears brighter than the other. The separation of each region is 4.9 Å. A model that

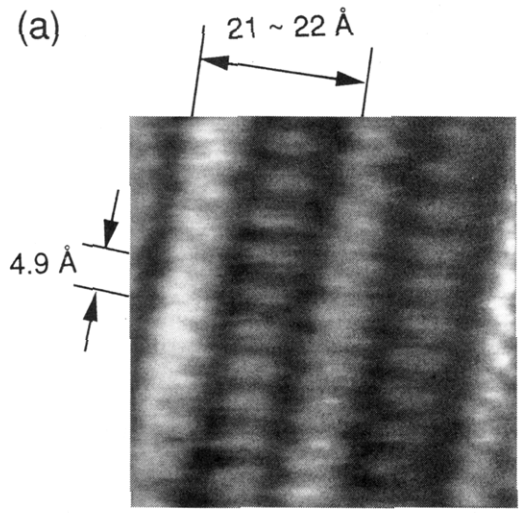

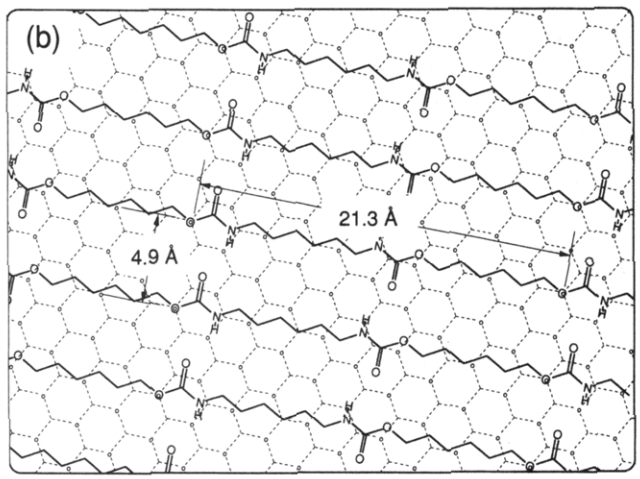

Figure 1. (a) STM image of (6,6)urethane on graphite. A region of strong current appears bright on this and all images presented in this paper. (b) Schematic drawing showing a model that is consistent with the STM image. A thick zigzag line indicates the ethylene part of the polymer. A dashed line is used to draw a graphite hexagonal lattice with a small circle on every other edge of hexagons denoting the strongly tunneling site.

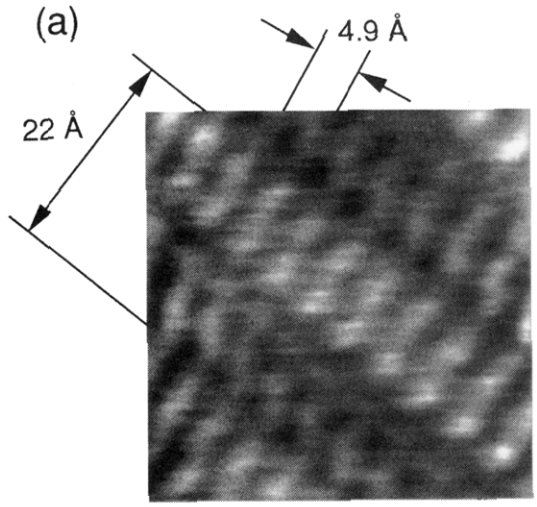

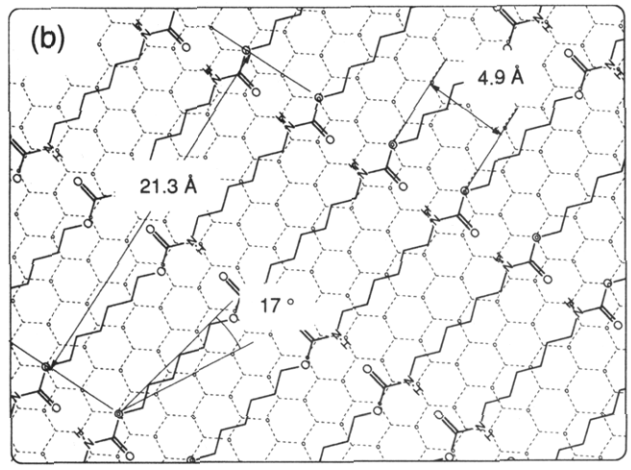

Figure 2. (a) STM image of (6,6)urethane, taken at a different location on the same sample as in other images of polyurethane. (b) Schematic drawing of an epitaxial structure that is consistent with the STM image. This chain orientation maximizes hydrogen bonding and places every monomeric unit in registry with the graphite lattice.

explains this image is schematically shown in Figure 2b. A polymer chain orients so that the fiber axis is rotated 17° from the $2\bar{1}\bar{1}0\rangle$ line. This rotation gives the predicted periods of 21.3 and 4.9 Å, in agreement with the actual image. Making one monomeric unit to be in registry with the graphite lattice results in the fiber identity period of 21.9 Å. Since each atomic species of the polymer chain in this orientation situates differently with respect to the graphite carbon atoms, the STM contrast should vary by every polymer atom. The streaked appearance is consistent with this consideration.

Figure 3a presents another image taken from the different location on the surface. This image differs from the previous two images by its disjoint positioning of bright regions. The periods are 21 and 12 Å, forming a rectangular pattern. There are other bright spots with different contrasts situated within this rectangle. Figure 3b shows a schematic of the most probable model. The all *trans* chains in $\langle 10\bar{1}0\rangle$ orientation are the same as the previous model shown in Figure 1b and produce the identity period of 21.3 Å. The present model differs from others by the relative direction of the adjacent chain defined by the urethane unit in that this is antiparallel while others are parallel. Note that hydrogen bonding cannot be made on every urethane unit in the anti-parallel orientation. Packing of the antiparallel chains on the flat surface to form a structure that has a lattice matching in every monomeric unit and is in a relatively close packed state results in another period of 12.3 Å and a rectangular placement of the urethane units.

The rotational angle of 17° in Figure 2b is quite unique. This is the only orientation that maximizes hydrogen bonding in every urethane unit and places every monomeric unit in line with the graphite lattice at the same time. This packing is also consistent with a logical extension of the triclinic crystal structure found for even numbered polyurethane in bulk.[16] The fiber identity period of 21.9 Å, however, differs from those of other models by 2%. Since the variation of this magnitude is within the experimental error commonly encountered in the bulk studies, we cannot determine whether one of our models is false or the polymer actually takes two different lengths. We think that this is within an elastic range of the polymer, since the mismatch only amounts to 0.1% for each atomic bond.

Polymerization-Induced Epitaxy of (6,6)Urethane. The XPS data and the highly aligned, periodic features of the STM images support the fact that a

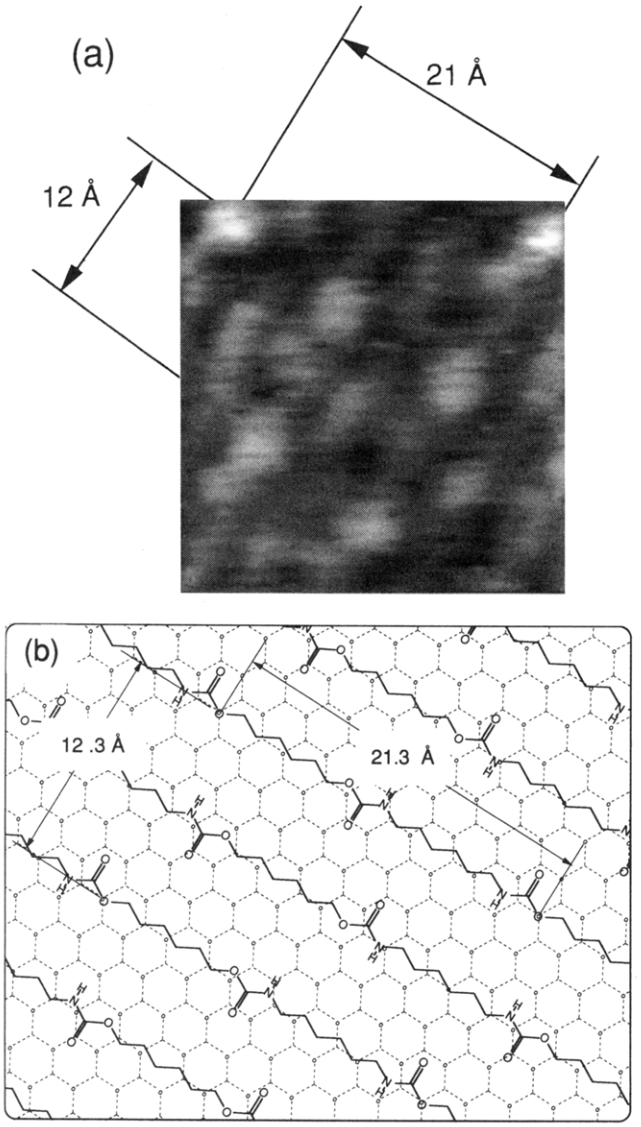

Figure 3. (a) STM image of (6,6)urethane. (b) Most probable model corresponding to the STM image. This model differs from the other by the anti-parallel packing of the chains.

crystalline form of (6,6)urethane is present on the graphite surface. Since the molecular models with a definite crystallographic relationship with the graphite lattice explain most of the STM images, it is an epitaxial film of (6,6)urethane on graphite.

We have also performed a controlled experiment. Another freshly cleaved graphite was immersed in a solution containing a preformed polyurethane under the same conditions as the polymerization experiment and was washed in the same way as before. No ordered structure was observed from this surface. Also, we could not observe any molecular images if the polymerization was terminated early so that only short oligomeric species that dissolved easily in solvent were produced. These facts indicate that polymerization is necessary to form the epitaxial film. Therefore, we conclude that an epitaxial film of (6,6)urethane is formed by PIE during the polyaddition reaction.

Epitaxial Structures of (6,10)Ester. This sample produced at least three different types of images from the same surface, shown in Figure 4a,c,d. Figure 4b belongs to the same type of image as Figure 4a. It is interesting to note the drastically different appearances of these images from those of polyurethane, although both polymers have approximately the same fiber identity period with the only difference being a methylene unit in place of an amide nitrogen. Due to the spatially nonsymmetric ester unit, it is difficult to relate the STM image with a molecular structure. No one-to-one correspondence between an ester unit and a bright region on the images was observed even in the simple polyesters such as poly(δ-varelolactone) and poly(ϵ-caprolactone).[3]

Figure 5 shows a higher resolution image of Figure 4a. This image is characterized by an alternating appearance of the elongated bright and dark regions to form a straight line of 21−22 Å repeating distance and 4.9 Å apart, running diagonally in this figure. These brighter regions also align in the other direction to form a short band. Then, there is a sudden shift of the position of this band along the straight line for every sixth line.

A schematic drawing shown in Figure 5b shows a model of planar zigzag polyester chains within the short band. In this figure, we have arbitrarily drawn the chain so that the alkoxy oxygen atom is located on the strongly tunneling graphite carbon only to make the relative orientation clear. Because of the difficulty discussed above, we cannot specify the exact position of polymer relative to the graphite lattice nor which portion of the chain corresponds to the bright feature. Thus, the model has an ambiguity in that the whole polymer lattice can be translated by an arbitrary amount either vertically or horizontally in this figure. Having the fiber axis rotated by an angle of 13° from the $\langle 10\bar{1}0\rangle$ line reproduces the model periods of 21.3 and 4.9 Å as calculated from the graphite lattice constant, in good agreement with the image. This orientation of the polymer lattice is geometrically the same as the second case of (6,6)urethane shown in Figure 2b. The fiber identity period becomes 21.9 Å in this model and is close to the bulk vlaue of 22.15 Å taken by the all *trans* conformation.[17]

The relative placement of adjacent chains in this model is not the most favorable one. From the consideration of dipole−dipole interactions as well as the interaction with the substrate surface, we expect that the ester groups should be placed as far apart as possible and the chains are oriented to have a lattice matching between a monomeric unit and the graphite. It is possible to construct such models by rotating the chain 42° from $\langle 2\bar{1}\bar{1}0\rangle$ or 43° from $\langle 10\bar{1}0\rangle$, producing the model STM periods of 14.5 and 14.9 Å, respectively. The STM images having the corresponding periods, however, have not been observed yet. The periodic shifting of urethane positions in every sixth chain along the fiber axis may be caused by the unfavorable chain orientations by the dipole−dipole interactions.

The upper right half of Figure 4a shows a disordering of the bright bands. This may be caused by a shifting of urethane units along the backbone direction slightly to make the next band incommensurate with the graphite lattice. This should cause every ester unit to have approximately the same contrast. This type of misfit is also seen at the line joining the arrows in Figure 4b. Although there is a possibility that this misfit may be caused by a crystalline misfit of the underlying graphite surface, we think that it reflects a domain wall of polymer lattice since the height (or contrast) difference is not seen across the border and the misfit is along the fiber axis.

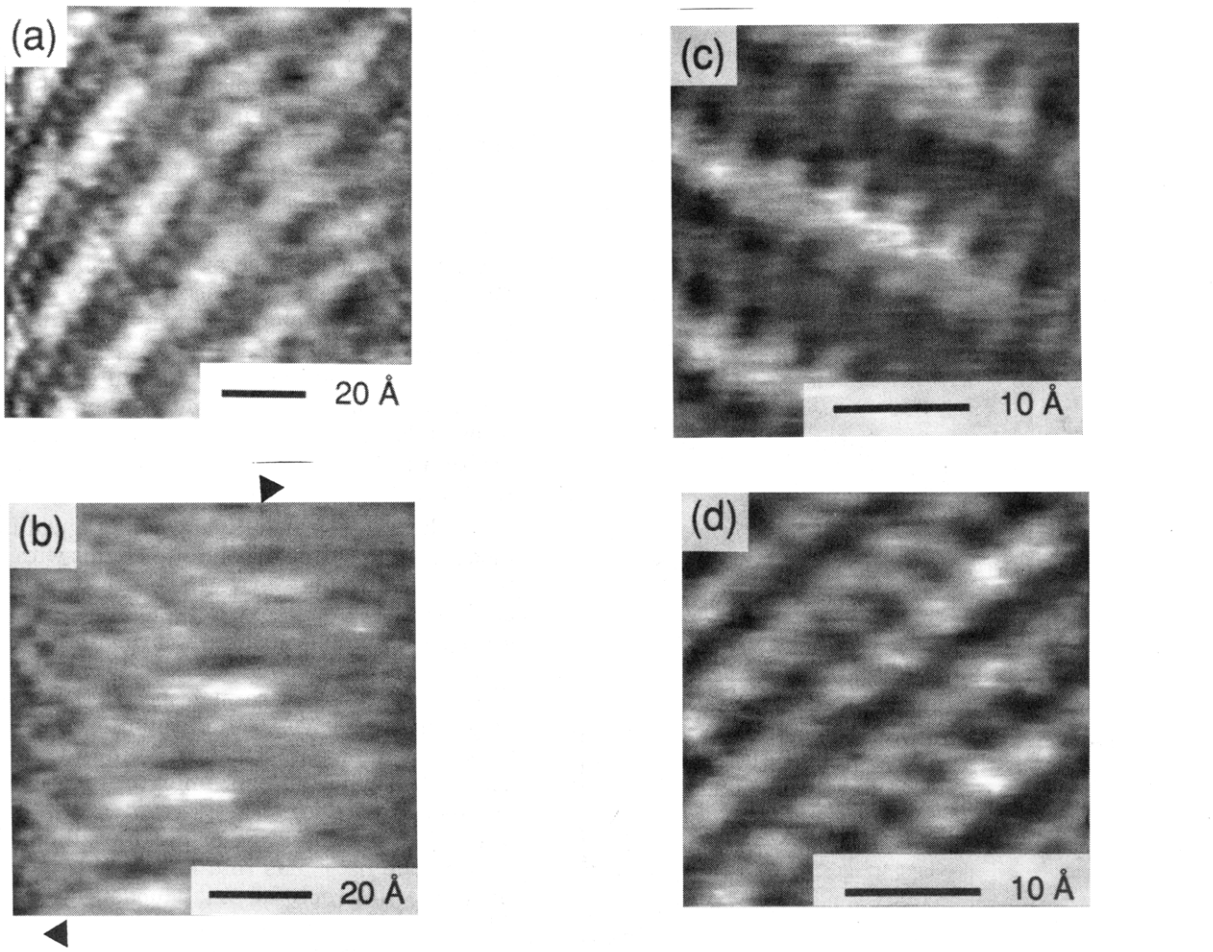

Figure 4. (a) STM image of (6,10)ester on graphite, showing a highly aligned array of polymers. There is a shift of relative chain position along the fiber axis in every sixth chain. A disturbance of this pattern resembling a double image at the upper right corner may be due to a shift of chains causing an incommensurate orientation. (b) Another STM image belonging to the same type as shown in (a). The bright short bands orienting diagonally in (a) are lying horizontally in this image. Here, the misfit occurs at the line connecting the arrows. (c) and (d) Other STM images of (6,10)ester. No models consistent with these images have been found.

We have not been able to find the models consistent with other images. Figure 4c has a feature of the bright regions, 4.4 Å apart, lining up to form the parallel lines of 23–24 Å width. A rectilinear alignment of bright regions is also seen in Figure 4d having 11.5–12 Å line separation and a 4.4 Å step. These figures may reflect the same polymer lattice in different orientations relative to graphite, since making every spot of Figure 4c have equal contrast results in the image resembling Figure 4d.

Epitaxial Structures of (6,T)Ester. Figure 6a shows one of at least two types of images observed in this polymer. The most characteristic feature of this image is that two crescent-shaped bright regions form a pair, making a butterfly-like feature, as clearly seen in Figure 6b. This feature is absent in the aliphatic polymers and may be linked to the aromatic ring. There are two distinct directions defined by the direction of cleavage in which butterfly-like shape points. Those pointing in the same direction are on a straight line and others pointing in the other direction also form a line in parallel with the other lines, and these two types of lines appear alternatively. The unit cell dimensions from the STM images are 15 Å and 11–12 Å, as indicated in Figure 6b.

Because the ester units are symmetrically attached to a benzene ring, a terephthalate unit as a whole gains symmetry. Thus, although we cannot specify which atom corresponds to a bright region, we can assume a butterfly-like feature corresponds to a terephthalate unit. Then, a model that reproduces the observed unit cell dimensions is given in Figure 6c. Again, we have arbitrarily drawn the chains so that an alkoxy oxygen atom coincides with the strongly tunneling graphite carbon, only to make the relative chain placement clear. Two different directions of butterfly-like features suggest an anti-parallel packing of the chains. Then, fully extended chains making 16.1° from $\langle 2\bar{1}\bar{1}0\rangle$ in the anti-parallel packing give the unit cell dimensions of 15.4 and 11.1 Å, as calculated from the graphite lattice constant. The fiber identity period is in excellent agreement with the bulk values of 15.4–15.74 Å.[18–21]

Contrary to the aliphatic polyesters, the presence of the terephthalate unit necessarily makes the direction of fiber axis deviate from the direction of the aliphatic segment. Thus, the anti-parallel packing results in placing every neighboring chain in nonequivalent position which respect to the graphite lattice. A unit cell contains two monomeric units but aligns with the graphite lattice by the rotation of 16.1°. This orientation also makes a close packed state of anti-parallel chains, as suggested by a bulk study.[19]

Figure 7a shows the seocnd type of images obtained from the same sample surface. It consists of an array of parallel lines 7–7.5 Å apart. Within a line is a ripple-

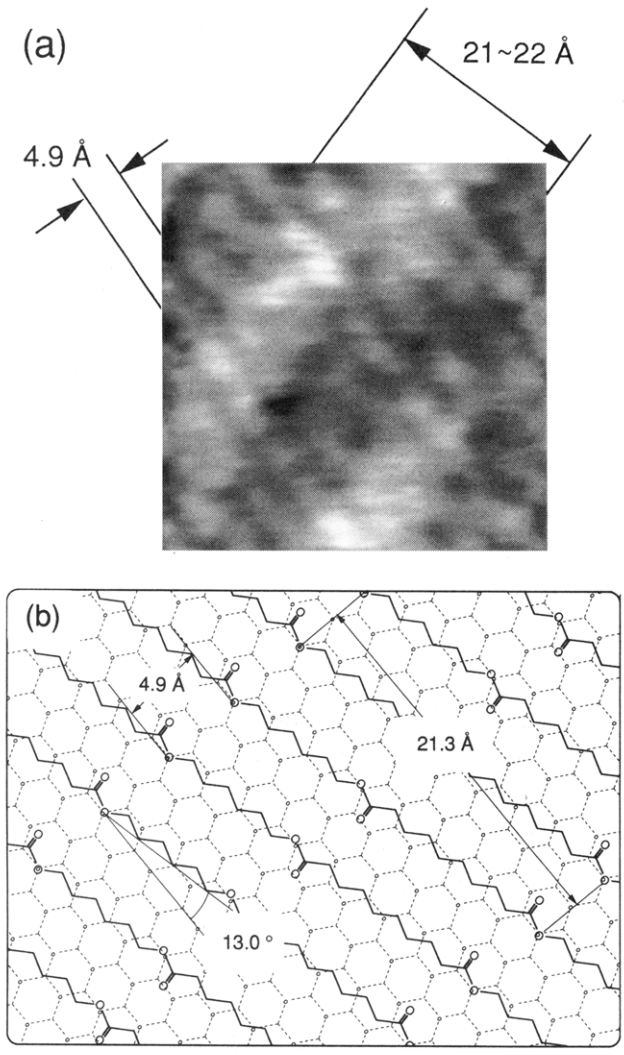

Figure 5. (a) High-resolution STM image of (6,10)ester, taken at the same location as in Figure 4a. (b) Schematic drawing showing a model that is consistent with the STM image.

like contrast modulation with a period of 11 Å. Although we have not been able to get a higher resolution image of this type to see if the butterfly feature is present, these ripples appear to point in the same direction on every line. A model for this image is the similar orientation of fully extended chains in 16.1° rotation, but in parallel packing, as shown in Figure 7b. In this case, every monomeric unit is in registry with the graphite lattice and should appear equivalently in the STM image. The periods of 10.7 and 6.9 Å from the graphite lattice constants agree with the actual image. This is also a logical extension of the triclinic structures found in bulk to the plane surface.[20,21]

STM Observation of (Butyne,10)ester. About 70% of the images obtained had a rectilinear pattern of a ladder-like feature, as shown in Figure 8a. Some of the images also exhibit moiré fringes on top of the ladder-like pattern. A high-resolution image shows that a ladder consists of a few streaked bright regions, 12 Å wide with a step of 4.4 Å, as depicted in Figure 8b.

Since no bulk study is available for this polymer, we estimate a fiber repeat of 19.6 Å for a fully extended chain using the standard bond angles and distances. At this moment, we have not been able to propose any structures that reproduce both periods yet. We present here a model that is consistent with other studies of epitaxial polymers. The most probable model that

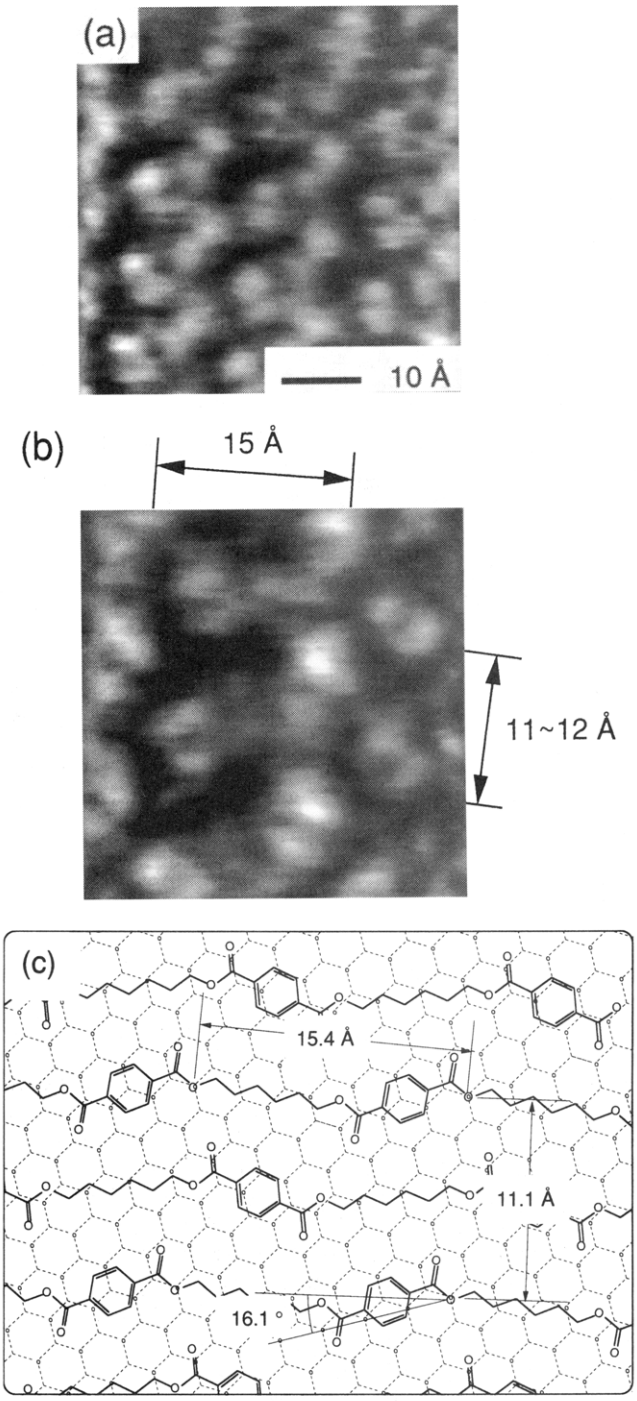

Figure 6. (a) One of two types of the STM images of (6,T)-ester, exhibiting a twisted ribbon-like feature not seen in the aliphatic polymers. (b) High-resolution image of (6,T)ester, belonging to the same type of image as in (a). The butterfly-like feature is unique to this polymer among other studies so far. (c) Schematic drawing of the epitaxial model of (6,T)ester. A comparison with the STM image indicates that the bright butterfly region corresponds to outside the benzine ring. The chains are packed in the anti-parallel orientation.

reproduces a longer period of 12 Å is schematically shown in Figure 8c. The fully extended chains rotate 19.1° from the $[2\bar{1}\bar{1}0]$ line in a parallel packing. Making every monomeric unit align with the graphite lattice gives a fiber identity period of 19.5 Å. Assuming the butyne units to be the bright regions on the images, the predicted periods are 12.1 and 6.5 Å. This paradox of an agreement in a long period but not in a short period has been seen in polylactones.[3] So far, this difficulty has been met on the polymers that contain

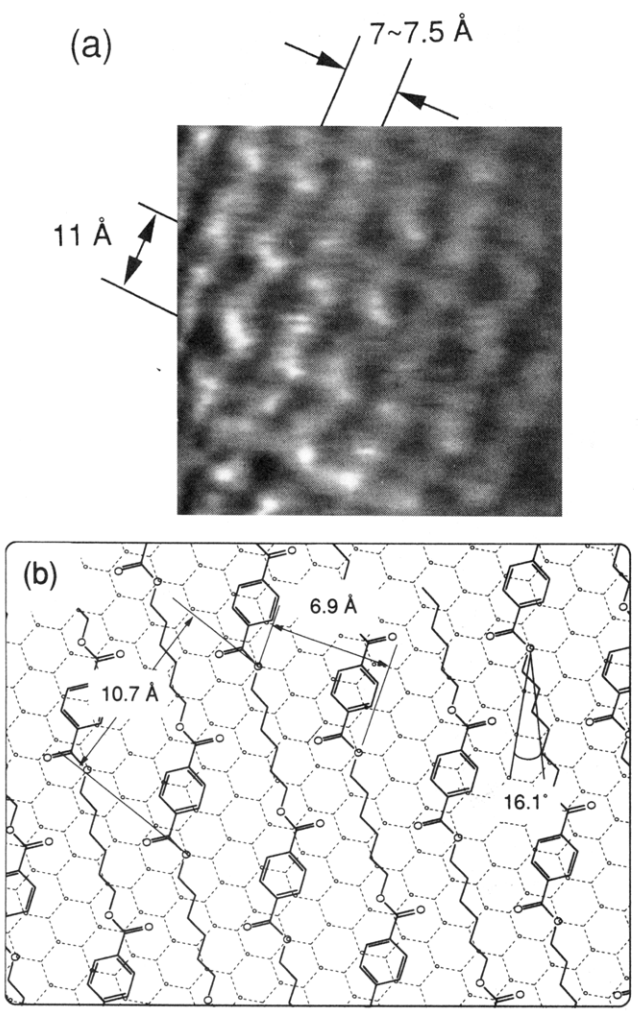

Figure 7. (a) Another type of the STM image of (6,T)ester, having a ripple on the parallel lines pointing in the same direction. (b) Model of (6,T)ester in the parallel orientation.

ester groups that are distributed over the surface in high density. In this case, the simplified procedure to analyze the STM images adapted here is no longer satisfactory and a quantum mechanical calculation is necessary to proceed further. Incidentally, the predicted values of short periods in polylactones were also 6.5 Å while the periods of about 4.5 Å were experimentally observed.

Polymerization-Induced Epitaxy of Polyesters. Because a freshly cleaved graphite always contains a slight amount of oxygen at its defects, oxygen is not a unique element from the polyesters. Nonetheless, we have observed by XPS an increase of oxygen content on the graphite surface after polymerization, which is consistent with the presence of polyesters on the surface. The highly ordered pattern of STM images with features characteristic of each polymer, the polymer structures that are consistent with the STM images, and the controlled experiments without polymerization indicate that the epitaxial films of (6,10)ester and (6,T)ester have been formed during polycondensation reactions. For (butyne,10)ester, we have shown that a crystalline film has been formed by the PIE process. A comparison with other esters suggests that there is a good possibility that (butyne,10)ester is also grown epitaxially.

Verification of PDMS Films on Graphite. Because crystallization at temperatures so far above the bulk melting point was not expected in the first place,

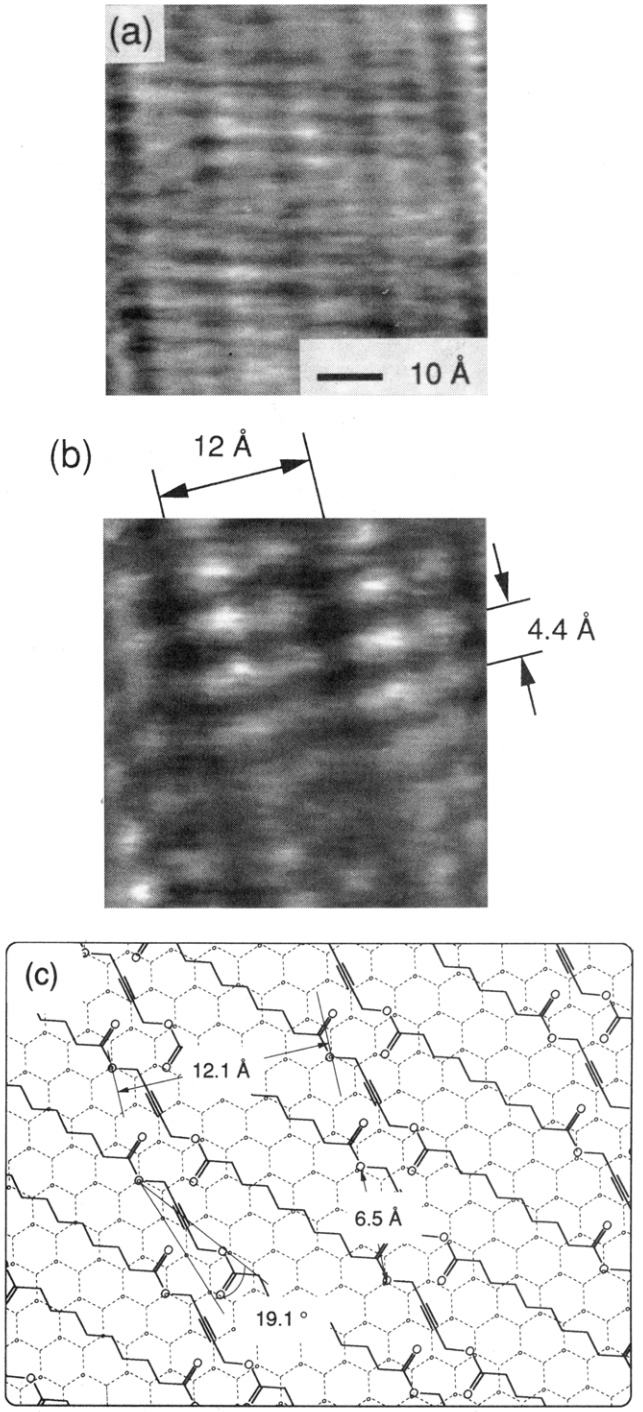

Figure 8. (a) STM image of (butyne,10)ester, characterized by an aligned laddle-like pattern. (b) High-resolution image of (butyne,10)ester. The images of this polymer are often modified by moiré fringes. (c) The most probable model of (butyne,10)ester for the STM image of (b). The agreement in the long period of 12 Å, but not in the short period of 6.5 Å vs 4.4 Å is also observed in another polyester study.[3]

we have repeated the same polymerizations and the STM experiments using the different graphite pieces and have confirmed the good reproducibility of results. This excluded a possibility of imaging graphite artifacts by STM. Typically, bulk PDMS obtained from the polymerization of D3 had a number average molecular weight of 44 000, as estimated from gel permeation chromatography and nuclear magnetic resonance. Differential scanning calorimetry of the same sample indicated a glass transition temperature of −126 °C and a melting point of −42 °C.

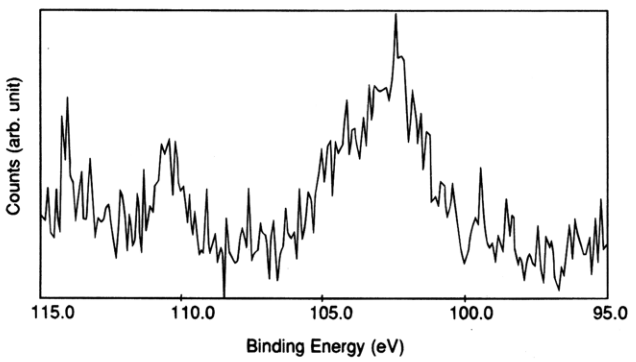

Figure 9. XPS spectrum of the graphite surface that has been subjected to polymerization of PDMS and has been washed rigorously by good solvents of the polymer. The low counts are expected from the coverage that has been seen in the STM experiment.

As shown in Figure 9, an XPS spectrum from the washed graphite sample exhibits a peak at ca. 102 eV, corresponding to the known Si_{2p} peak of PDMS. It is not clear if two unidentified satellite peaks at higher energies have any relation to the crystalline film. The O_{1s} peak at 533 eV increased after polymerization and washing routines. No lithium or potassium from other reagents was detected within experimental error. These data are consistent with the presence of PDMS on the surface even after rigorous washing. Also, the STM images obtained from the D4 sample are indistinguishable from that of the D3 sample. Since the final form of polymer is the only common factor from these reactions, the imaged molecular film should belong to the same polymer. These observations support that the film remaining on the graphite surface after washing is PDMS.

STM Observation of PDMS. Of over 100 images examined in detail, more than 80% have a feature of ladder-like alignment of elongated rods, as shown in Figure 10a. The D3 sample surface was covered more by the region exhibiting this type of image than the D4 under the referenced polymerization conditions. Figure 10b indicates the principal periods, corresponding to a rod of 4.4 width and 11.7 Å length on the average. These periods are not associated with the observed diffraction periods of bulk PDMS ($a = 13.0$ Å, $b = 8.3$ Å (fiber axis), $c = 7.75$ Å).[22] Under the situation that the structure of bulk PDMS is not known with certainty and the number of atoms involved in theoretical calculation is expected to be prohibitively large, it is not possible to reduce the molecular structure from these images.

Thus, we compare the present results with the previous studies of bulk polysiloxanes. A monomer repeat can be estimated to be 2–3 Å from the value of 2.5 Å taken by poly(diphenylsiloxane).[23] Then, the unit cell in the STM image must contain more than one monomer unit. Since the all *trans* chain, which is thought to be of low energy, gives circular forms, a rectilinear pattern of the image indicates that the chain should deviate from the all *trans* conformation. As discussed by Flory,[24] a weak preference of *trans* over *gauche* is due to the interaction between nonbonded methyl groups and not by the siloxane bond. Here, a chain conformation may deviate from the 6_1 helix proposed for bulk PDMS because of the additional interactions of the methyl group with the graphite surface. This is consistent with the observation that the STM image cannot be explained by simply placing the proposed bulk helix on top of graphite. Regardless of the structures taken on the graphite surface, the STM images showing well-defined periodicity indicate that the chains are placed with two-dimensional positional order.

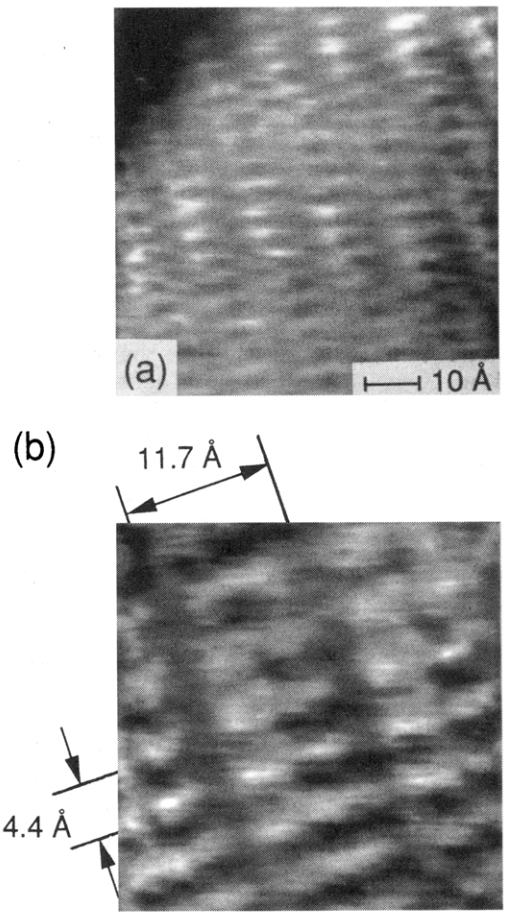

Figure 10. (a) STM image of PDMS on graphite. A rectilinear alignment of the rodlike structures is the most dominant feature among the images obtained from all samples. This particular image shows a region near the film edge appearing as a dark region at the upper left corner, which is not stable against a prolonged scanning. (b) High-resolution image of PDMS. Further zooming reveals that each rod in this image is consisted of several bright spots, forming a rotated "L" shape feature. The shown periods are the averages from all other images.

Once formed, the ultrathin film of PDMS showed good chemical and physical stability. We could repeatedly obtain the molecular images of the same pattern even after leaving the sample in ambient conditions over a period of months. During the STM experiments, a force exerted by the scanning tip on the film might reach the same order of magnitude as an onset of plastic deformation[25] and becomes stronger as the tip approaches the sample more closely. Although the film can be damaged at the tip–sample distances corresponding to the voltages below 0.4 V at 200 pA, reproducible imaging at higher voltages implies that the film can still withstand a considerable stress.

Crystalline PDMS Films Formed during Polymerization. A fresh graphite sample immersed in a preformed PDMS solution and washed similarly showed no sign of an ordered structure. Thus, this molecular film with a high degree of positional order is formed through polymerization. Since both D3 and D4 involving different chemistry give identical structures, a possibility of chemisorption to the graphite surface is very low. Also, an absence of geometrical pattern suggesting cyclic macromers implies that it is not a

crystallization of cyclic oligomers. Therefore, we conclude that although we could not specify any definite crystallographic relationship between the PDMS film and the graphite surface, a solid PDMS film with extremely high positional order has been produced by the same process as PIE. This means that the observed state has been formed in a good solvent at 160 °C above or in melt at 200 °C above the bulk melting point.

Discussion

Structures Permitting Epitaxy. As an ultra-thin crystalline film, it is observed that the polymer lattice is described by two unit vectors defined on the film plane. We have not considered the chain packing whereby the plane defined by the *trans* zigzag backbone or the aromatic ring is not laying perfectly flat on the graphite surface. Otherwise, close packing places chains incommensurate with the graphite, and the varying distances of each atom on the chain from the substrate surface have an unpredictable effect on the STM images. It is highly interesting to note that all polymers we have analyzed so far have a reflection symmetry by the film plane, i.e., the structures on the side facing the graphite are the same as those on the one facing the air.

This question of symmetry arises, partly because we have limited our study to a molecularly thin crystalline film. Since STM can be applied only to ultrathin films permitting tunneling, the sample must be prepared accordingly. A rigorous washing of the surface after polymerization is necessary for STM experiments but may result in a loss of thick crystalline films also. Thus, the structures presented here belong to the part of the films that are not dissolved by regular washing conditions and that have had soluble layers on top at the termination of reaction. The symmetry problem should be treated differently for the three-dimensionally grown crystals.

Two factors on their structures are common to all polymers, namely, lattice matching and close packing. In polymer epitaxy where each molecule is a repetition of a monomeric unit, which in turn is made of covalently bonded atomic units, it is not obvious which level—atomic, monomeric, or larger unit—of lattice matching is most important. While many structures presented in this paper show a lattice matching at the monomer level, polyethers show that every methylene unit is commensurate in one modification while many monomeric units as well as a number of chains are involved to satisfy a lattice matching condition in other forms.[2] In the hydrogen-bonded systems, a two-dimensional network by the bonded pairs from adjacent chains needs to be considered in place of alignment of an individual chain.[3,4] Thus, two-dimensional placements of chains as a whole need to be considered for the relevant level of lattice matching.

Interactions with the surface should also influence what level will be most relevant for polymer epitaxy. Graphite, however, constitutes a very special kind of surface. The basal plane is made of carbon atoms packed in a hexagonal lattice, resulting in lattice parameters that are close to those of most organic bonds. Due to the polymers intrinsically periodic nature, a macromolecule can find some orientations in which either monomeric or integer multiples of monomeric units satisfy lattice matching. The lattice parameters of polymers can be varied a little to aid this by only minute changes in bond angles and distances of each bond of elastic organic molecules. Graphite is also characterized by a two-dimensional, complete spreading of π-electron resonance, stabilizing many chemical species. This inert terrace extends over several hundred nanometers without any surface defects. The defect free, nonionic surface makes only van der Waals interactions relevant for the macromolecules. While a small molecule is affected by a detail of exact interaction on the graphite surface,[26] the interactions on each atom are integrated on a long-chain polymer molecule and may be smoothed out to some extent.[27] In this respect, we see a large allowance in structures that can be epitaxially grown on the graphite surface. At the same time, this may induce polymorphic films.

While commensurability may be sufficient, it is not a necessary condition for the epitaxial growth by PIE. There are more than 30% of the images left for each polymer that we cannot explain. One of the problems is a difficulty in predicting the features on the STM images of polymer lattices that has no lattice matching at all levels with the graphite lattice. Also, it is difficult to predict an image of multilayered films, regardless of its registry. Thus, there is a good possibility that those unexplained images contain incommensurate structures. Also, the domain walls in (6,10)ester as seen in Figures 4a and 4b may be taken as an indication of weak incommensurability.

The importance of an ability to form a close-packed state in two dimensions is evident from the present study. Both parallel and anti-parallel orientations of neighboring chains were observed from the same sample surface on many polymers. These variations are hardly seen in the bulk solid state of the polymers. This implies that the relative chain packing has no effect on polymer epitaxy on graphite under the conditions conducted in this study. The polymorphic growth of the aliphatic polymers and the chains placed in a nonequivalent orientation in (6,T)ester may also be taken as an indication that the film can be grown as long as molecules can be close packed on the surface. Thus, close packing in two dimensions seems to be the critical factor on the molecular structures permitting the PIE growth, rather than other conditions required by the intermolecular interactions and the molecule–surface interactions.

This point is further supported by the experimental observation that the monomers having a chiral center, such as methyl methacrylate and vinyl chloride, fail to produce any crystalline film on graphite upon nonstereospecific polymerizations.[28] These atactic polymers cannot form bulk crystals with a high degree of positional order due to steric reasons. The restriction imposed by stereoregularity on the epitaxial growth signifies an importance of polymer structures that permit close packing in two dimensions.

It is worth mentioning that we have often found a patch of films at the middle of the flat terrace away from any surface defects of graphite. In fact, very few numbers of films were seen to be near the graphite defects, such as steps, pits, or protrusions. This provides important information concerning the PIE mechanism that the substrate defects do not act as initiation sites nor as anchoring points for the film formation and that flat, homogeneous surface is rather suited for epitaxial growth by PIE.

Chemical Characteristics of Polymerization-Induced Epitaxy. The experimental observations concerning polymerization are summarized as follows:

(1) PIE requires the polymerization process. (2) The polymerization must proceed to some extent. (3) It is completely independent of the polymerization mechanism. (4) The polymer film is chemically identical to the polymer grown in solution. (5) The substrate can be introduced either before or after the start of the reaction. (6) Film growth is independent of the solubility of grown polymers in solution. (7) A wide range of temperatures and reactant concentrations is allowed for film formation.

(1) and (2) imply an existence of a critical molecular length for a successful film growth. (3) and (4) indicate that graphite does not participate in the chemical reactions at all and that the reaction responsible for the chain growth of the crystallized film is the same as the one proceeding in solution. (5) and (6) suggest an importance of soluble oligomers at the beginning and during the growth stage of PIE. (3) also implies that an exact molecular weight distribution of oligomers is of less importance. Together with (7), we see that PIE is not an ordinary crystallization process nor adsorption of polymers in solution.

Model of Late Stage of Polymerization-Induced Epitaxy. The following discussion is only relevant for formation of the first few layers on the substrate surface. A crystal growth on top of the surface layers should involve processes seen in ordinary crystallization, such as reentry of chains, fold, and slides.[8,29] We will not consider this three-dimensional crystalline growth, since our structural studies have been based on the STM observations which can only probe the surface layers.

Also, it is important to recall that the actually observed samples have undergone both PIE and washing treatments. This washing has been performed to the extent (and usually further) that ordinarily adsorbed molecules are no longer detectable as the reproducible peaks by XPS. Thus, any materials that are formed by reversible adsorption or ordinary crystallization should be rinsed away at this stage. This implies that these processes acting independently cannot explain the PIE mechanism.

As demonstrated in this paper, the polymer that can take a structure permitting a close packed state (may consist of multinumbered chains) in the flat planar geometry qualifies for PIE. Here, we propose a tentative model based on a view that the crystallographic attachment of a chain takes place concurrently with the chain growth. One of the other possibilities is a formation of microcrystals by physical gelation of intermediate polymer species.[30] It is, however, difficult to relate physical gelation with the polymerization process presently. Since the polymerization process is the most unique and essential feature of PIE, we consider the PIE mechanism from a point of view of the reaction process.

Presently, an initial stage of PIE is largely unknown. As discussed before, we think that oligomers play a key role at this stage. Under the temperatures and the kind of solvents that we have performed the reactions, any aggregates formed at an initial stage of PIE should be dissolved completely and the process should result in ordinary adsorption if it were without polymerization. Also, the process at this stage should allow a variety of epitaxial structures to be formed simultaneously on the same surface. Thus, some collective behaviors of growing oligomers driven by statistical fluctuation may be involved at the initial stage of PIE.

Once the formation of crystalline film is initiated, a model of crystalline growth at a later stage can be proposed, at least qualitatively. Very few numbers of crystalline defects within a grown film indicate an absence of reactions taking place within the crystalline part of films. The chemical reactions, therefore, should occur at the chain segments that are free from the crystal body. The film growth that is independent of chain growth mechanisms and the formation of ordinary polymers as expected suggest that the free segments of growing crystals should extend into the solution phase long enough to behave as if it is a part of ordinary reacting segments in solution. Another model with a growing end very close to the crystalline part of films on the surface and having a reaction on the surface is highly unlikely for steric reasons and by the following observations. The chain growth is monomerwise for chain polymerization but is not uniform in step polymerization. The reacting segments having any number of monomeric units are added to the free segments and can still be incorporated into the film. This indifference means that the chemically growing ends are not affecting the crystallographic attachment directly and, therefore, are away from the region being crystallized. The entropic polymerization of PDMS as discussed below and the STM finding of nonstructured regions existing around the crystalline area are also consistent with this picture.

The way that the free segments are incorporated into the crystalline region may depend on the chain packing as well as the dynamics involving chain folding and slides. This attachment process should, however, take place frequently or fast enough so that the length of a free segment is not too long to act as a polymeric chain by itself. This comes about by the facts that no epitaxial growth has been evidenced by preformed polymers under the present experimental conditions and that the epitaxial films can be obtained even from the systems where grown polymers precipitate during the reactions. Thus, the length of a free segment should not be too long to cost a large entropic loss during attachment. The chain growth mechanism of step polymerization suggests a possibility that incorporation of free segments into the crystalline region needs not be monomerwise but may involve addition by a segment of oligomeric length or by a batch of segments.

This relates the growth mechanism to the PIE kinetics. The proposed mechanism implies that the crystallographic attachment rate should be faster or comparable to the chain growth rate, so that the crystallization rate is about the same as the polymerization rate. Because we do not know the crystallization rate of PIE in practice, control of reaction conditions to slow the chain growth down is an effective means of encouraging the crystal growth.[2]

The crystal growth on the same level of surface layers can be terminated by several reasons. Obviously, quenching of polymerization will cut the material supply and stop the growth. Secondly, if the crystalline region continues to grow till it comes close to neighboring films, a free segment cannot be fit into the free space on graphite and is sterically rejected.[4] As polymerization continues, this may result in either a tethered chain or development of multilayers crystals. Also, if polymerization produces a heterogeneous junction at the growing end, such as branching or cross-linking, this junction may act as a structural defect and may not be incorporated into the crystalline region. Experimentally, we

have often observed only a small patch of films if polymerization with many possible side reactions has been employed. Finally, there is a possibility of film instability caused by nonsymmetric structures. As discussed in the previous section, a highly crystalline film without a reflection symmetry about the film plane may not be stable due to different surface energies on each face. A gradient of surface energy should result in a disturbing force perpendicular to the planar film. We expect that this effect becomes more significant for a film with a larger area.

PIE Process of PDMS. According to the proposed mechanism, the length of free segments is determined by thermodynamics of the reacting system. A peculiar feature of PDMS is that polymerization of PDMS is accompanied by no change in enthalpy but by an increase of entropy.[31] Thus, the length of a free segment must be long enough to provide entropy in order to drive the reaction forward. This entropic gain in polymerization must be balanced by the free energy of crystallization. Since a crystalline film has been obtained well above the bulk melting point, it may be necessary to introduce surface thermodynamic quantities to describe the energy balance. Here, we only comment on a possibility of providing a large energetic contribution to the crystallization process.

Due to the highly ionic character of the siloxane bond, the polymer intrinsically has a potential to be thermally stable. One of the major factors that prevent PDMS from crystallizing with a high positional order is the very low rotation barrier of the SiO bond which amounts to no more than a few hundred calories per mole.[24] Thus, if some larger side groups are introduced to the siloxane bond to sterically discourage the rotational motion, melting temperatures as high as 220 °C for poly(diphenylsiloxane)[32] and 100–200 °C for poly(dipropylsiloxane)[33] can be observed. In the present case, we think that there exists a molecular conformation of PDMS on a flat surface such that even the dimethyl group is enough for restriction of the rotational motion. The STM images correspond exactly to this conformation. Then the question is how this state has been achieved. The present experiment shows that a sequential attachment of the chain segment confined near a strictly planar surface can lead to the desired conformation. Since an ordinary crystallization process in three dimensions does not lead to such a state, the crystallization process as well as the equilibrium state may be of strongly two-dimensional character.

The proposed mechanism in the later stages of PIE can be considered as essentially a crystallization of oligomeric species on a solid surface. Because the oligomeric free segment of the crystallizing chain is also a growing end of the polymerizing chain, the process effectively results in crystallization of polymers at the end. This process, then, can be viewed as a crystallization process of preformed polymer molecules in solution or in melt where only the chain segment close to the crystallizing region is relevant to the process and the rest of the free chain away from this region behaves totally independent and has no physical significance to any processes. Under ordinary crystallization of polymers where the space available to the crystallizing chain next to the surface is three dimensions, the free part of the chain interacts with all its surroundings and entanglement takes place. If macromolecules are confined in the close vicinity of a flat surface under a suitable temperature and a solvent to cancel all relevant interactions with surroundings (may not be the same as a bulk ϑ condition due to the presence of a surface), individual molecule segregates and crystallizes as suggested above. In this respect, PIE may represent a crystallization process of polymers in two dimensions.

Conclusions

Epitaxial growth of polymers during polymerization reactions is shown to be completely independent of the type of polymerization. A vast number of polymers have the possibility of epitaxial growth if they can be synthesized in solution. A qualification for PIE is that a polymer should be able to take a molecular structure that permits close packing in the flat planar geometry. Graphite is one of the most general substrates that allows various polymer structures, even though it may result in polymorphic crystals. Extremely high positional order of monomeric units in an epitaxial film may be taken as an advantage to functionalizing the polymer film, by using standard chemical techniques and laboratory apparatus for solution polymerization.

STM is proven to be a very powerful technique for characterizing the ultrathin polymer film, since it is a difficult task to evaluate structures of a monolayer made of small atomic numbered atoms by other techniques. Even then, the quantum nature of tunneling electrons makes the image analyses too difficult to elucidate structures of all epitaxial films. We expect increasing difficulty as the chemical complexity of polymers increases. A control of the unit cell dimensions by incorporating different spacer elements through polymerization should help in the image analyses.

We hope to get more quantitative data to test the proposed mechanism. To proceed further, it is essential to specify a driving force, corresponding to supercooling in the case of ordinary crystallization, for the present epitaxial growth.

Acknowledgment. We thank M. Suzuki for assisting with the STM measurements and Supermolecules Project—JRDC for kindly letting us use the XPS.

References and Notes

(1) Sano, M.; Sasaki, D. Y.; Kunitake, T. *J. Chem. Soc., Chem. Commun.* **1992**, 1326–1327.
(2) Sano, M.; Sasaki, D. Y.; Kunitake, T. *Macromolecules* **1992**, *25*, 6961–6969.
(3) (a) Sano, M.; Sasaki, D. Y.; Kunitake, T. *Proc. Jpn. Acad.* **1992**, *68B*, 87–89. (b) Sano, M.; Sasaki, D. Y.; Yoshimura, S.; Kunitake, T. *Faraday Discuss. Chem. Soc.* **1994**, in press.
(4) Sano, M.; Sasaki, D. Y.; Kunitake, T. *Science* **1992**, *258*, 441–443.
(5) Sano, M.; Sasaki, D. Y.; Kunitake, T. *Langmuir* **1993**, *9*, 629–6631.
(6) Sano, M.; Sandberg, M. O.; Yoshimura, S. *Langmuir* **1994**, *10*, 3815–3819.
(7) For instance, Takahashi, A.; Kawaguchi, M. In *Advances in Polymer Science*; Springer-Verlag: Berlin, 1982; Vol. 46, pp 1–65.
(8) For instance: Armitstead, K.; Goldbeck-Wood, G. In *Advances in Polymer Science*; Springer-Verlag: Berlin, 1992; Vol. 100, pp 219–312.
(9) Mauritz, K. A.; Baer, E.; Hopfinger, A. J. *J. Polym. Sci., Macromol. Rev.* **1978**, *13*, 1–61.
(10) Odian, G. *Principles of Polymerization*; Wiley: New York, 1981; pp 102–109.
(11) For a recent review, see: *J. Vac. Sci. Technol. B* **1994**, *12*.
(12) Hölle, H. J.; Lehnen, B. R. *Eur. Polym. J.* **1975**, *11*, 663–667.
(13) Grubb, W. T.; Osthoff, R. C. *J. Am. Chem. Soc.* **1955**, *77*, 1405–1411.
(14) Sautet, P.; Joachim, C. *Jltramicroscopy* **1992**, *42–44*, 115–121.

(15) Fisher, A. J.; Blöchl, P. E. *Phys. Rev. Lett.* **1993**, *70*, 3263–3266.
(16) Saito, Y.; Nansai, S.; Kinoshita, S. *Polym. J.* **1972**, *3*, 113–121.
(17) Kanamoto, T.; Tanaka, K.; Nagai, H. *J. Polym. Sci.* **1971**, *9*, 2043–2060.
(18) Bateman, J.; Richards, R. E.; Farrow, G.; Ward, I. M. *Polymer* **1960**, *1*, 63–71.
(19) Joly, A. M.; Nemoz, G.; Douillard, A.; *Makromol. Chem.* **1975**, *176*, 479–494.
(20) Hall, I. H.; Ibrahim, B. A. *Polymer* **1982**, *23*, 805–816.
(21) Palmer, A.; Poulin-Daudurand, S.; Revol, J.-F.; Brisse, F. *Eur. Polym. J.* **1984**, *20*, 783–789. Brisse, F.; Palmer, A.; Moss, B.; Dorset, D. Roughead, W. A.; Miller, D. P. *Eur. Polym. J.* **1984**, *20*, 791–797.
(22) Damaschun, V. G. *Kolloid-Z.* **1962**, *180*, 65–67.
(23) Babchinitser, T. M.; Kazaryan, L. G.; Tartakovskaya, L. M.; Vasilenko, N. G.; Zhdanov, A. A.; Korshak, V. V. *Polymer* **1985**, *26*, 1527–1530.
(24) (a) Flory, P. J. *Statistical Mechanics of Chain Molecules*; Wiley: New York, 1969; pp 174–180, 392–396. (b) Flory, P. J.; Crescenzi, V.; Mark, J. E. *J. Am. Chem. Soc.* **1964**, *86*, 146–152.
(25) Woodward, J. T.; Zasadzinski, J. A. *Langmuir* **1994**, *10*, 1340–1344.
(26) See, for instance: Birgeneau, R. J.; Horn, P. M. *Science* **1986**, *232*, 329–336. Kim, H. K.; Zhang, Q. M.; Chan, M. H. W. *Phys. Rev. B* **1986**, *34*, 4699.
(27) Hentschke, R.; Schürmann, B. L.; Rabe, J. R. *J. Chem. Phys.* **1992**, *96*, 6213–6221.
(28) Unpublished results. Stereospecific polymerizations of these monomers have not been performed.
(29) Hirosaka, M. *Polymer* **1990**, *31*, 458.
(30) de Gennes, P. G. *Scaling Concepts in Polymer Physics*; Cornell University Press: Ithaca, NY, 1979.
(31) Lee, C. L.; Johannson, O. K. *J. Polym. Sci., Polym. Chem. Ed.* **1966**, *4*, 3013–3026.
(32) Liebau, F. *Acta Crystallogr.* **1961**, *14*, 1103–1109.
(33) (a) Peterson, D. R.; Carter, D. R.; Lee, C. L. *Macromol. Sci., Phys.* **1969**, *B3*, 519. (b) Wunderlich, B. *Macromolecular Physics*; Academic Press: New York, 1980; Vol. 3, Table VIII.6.

MA945013+